Multicast MMSE-based Precoded Satellite Systems: User Scheduling and Equivalent Channel Impact

Eva Lagunas*, Vu Nguyen Ha*, Trinh Van Chien†, Stefano Andrenacci‡, Nicolò Mazzali§
and Symeon Chatzinotas*
*SnT - University of Luxembourg, Luxembourg
†School of Information and Communication Technology (SoICT), Hanoi University of Science and Technology, Vietnam
‡SES S.A., Luxembourg
§ESA - European Space Agency, The Netherlands
Corresponding Author: eva.lagunas@uni.lu

***Abstract*—Very High Throughput Satellite (VHTS) systems are characterized by a multi-beam footprint covering wide areas and providing service to large numbers of users. Multicasting comes naturally to exploit the multiuser diversity in VHTS systems, where the data of different users are multiplexed in a single PHY frame. Following the DVB-S2(X) standard, the resulting PHY frame is encoded using a single codeword. The latter brings some practical implementation challenges when precoding is considered, as the precoder can no longer be designed on a user-by-user basis. Avoiding overambitious and impractical precoding designs, our work focuses on the low-complexity MMSE-based precoding, which has been considered as the baseline for early satellite over-the-air precoding tests. While the multicast scheduling has been widely investigated in the literature, we will show in this work that its performance is significantly impacted by the equivalent multicast channel calculation. Therefore, in this paper, we analyze and report the impact of the user scheduling (i.e., selection of users to be multiplexed together in a single PHY frame) as well as the methodology employed for the equivalent multicast channel considered for the precoding computation.**

***Index Terms*—VHTS, precoding, multicast, user scheduling**

I. Introduction

Although there is a lot of discussion about future lower-orbit constellations, geostationary (GEO) satellite systems still represent nowadays the most competitive and commercially available solutions offering high-speed broadband services over wide areas of the globe. In fact, key satellite operators have made strategic investments in next-generation GEO high-throughput satellites (HTS) with the objective of bringing exceptional broadband to key industry verticals such as telecom, energy, government, maritime and cloud [1], [2].

GEO HTS are typically deployed in high frequency bands (Ku or Ka band), which allow the satellite payload to be equipped with high directive antennas and to generate the so-called multibeam footprint, i.e., a plurality of user beams ($>$100) over a region of interest (see Fig. 1 for a typical multibeam footprint example). The narrow spot beams allow several beams to reuse the same spectrum resource. The conventional reuse factor is known as 4CR (four color reuse, resulting from two orthogonal frequency blocks and two polarizations). However, this conservative spatial frequency reuse, which avoids adjacent beams using the same frequency, imposes severe limits to the achievable throughput [3].

With the aim of pushing the limits of the achievable throughput and reducing the cost per transmitted bit, more aggressive frequency reuse has been considered in [4], [5]. When adjacent beams operate on the same frequency resource, the co-channel inter-beam interference becomes unbearable claiming for advanced interference mitigation techniques [6], [7]. Among the different options, the Regularized Zero-Forcing (RZF) precoding [8] is the most popular in the satellite communications community due to its low-complexity design and performance [9]–[11]. The RZF design is typically known as minimum mean-square error (MMSE) precoding, because of the similarities between transmitting beamforming in the downlink and receiving beamforming in the uplink [7].

The user scheduling has been shown to have a significant impact on the GEO satellite MMSE-based precoding performance (see Figure 5 of [12]). MMSE-precoding relies on channel matrix inversion and depending on which users are scheduled, the resulting matrix may turn out to be poorly conditioned, reducing the precoding gain [13]. Targeting semi-orthogonality among the channels of the scheduled users, there are two prominent design methodologies: (i) employing a cosine-similarity metric to account for such orthogonality [13]–[15], or (ii) considering the geographical location of the users (which is equivalent to the Euclidean Distance applied to their channel vectors) [16], [17].

In this paper, we address the *multicast* scheduling impact on MMSE-based precoded systems. *Multicast* within the context of GEO HTS refers to the fact that data bits intended to different users are multiplexed together within a single codeword in the DVB-S2 physical layer frame (PLFRAME), which are subsequently interleaved. For this reason, the MMSE-based precoding cannot be designed on a user-by-user basis [4]. Few works in the literature have addressed this issue in a pragmatic way, by simply calculating an equivalent channel vector representing the set of multicasted users within a beam (e.g., arithmetic mean applied directly to the channel coefficients [18], or arithmetic mean applied separately to phase and magnitude of the channel coefficients [15]). In this work, we present for the first time two new methodologies for equivalent

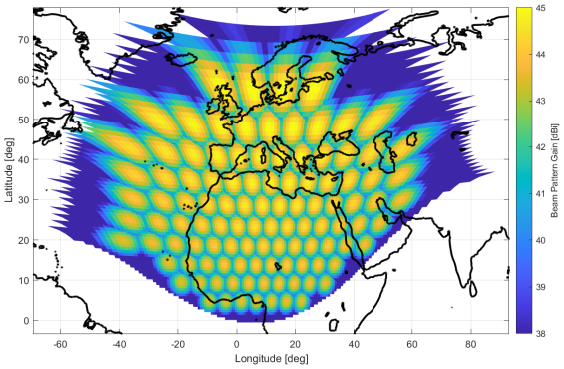

Fig. 1. Considered GEO multibeam footprint pattern with $N = 108$ beams.

channel calculation: (i) a phased-normalized equivalent channel (initially studied in ESA Optimus project [19]); and (ii) an upper-bound method emulating a virtual user terminal by averaging geographical coordinates of the multicasted users. Furthermore, this work compares and evaluates for the first time different multicast scheduling techniques combined with different equivalent multicast channel methodologies.

The remainder of the paper is organized as follows. In Section II, we present the considered system and channel model. Section III goes into the details of the different techniques proposed for the equivalent multicast channel calculation. Section IV briefly presents the different user scheduling alternatives. Section V presents the numerical evaluation and the paper is concluded in Section VI.

Notations: Throughout the paper, a capital bold letter such as $\mathbf{A}$ represents a matrix, and a lower case bold letter $\mathbf{a}$ represents a vector. The superscripts have the following meanings: $(\cdot)^H$ is the conjugate transpose of a matrix, and $(\cdot)^{-1}$ is matrix inversion. The function $\langle \mathbf{a}, \mathbf{b} \rangle$ denotes the dot product between vector $\mathbf{a}$ and vector $\mathbf{b}$, and $\|\mathbf{a}\|$ denotes the Euclidean norm of vector $\mathbf{a}$.

II. System Model

Let us assume the forward link of a bent-pipe transparent GEO multibeam satellite system. The beam footprint on Earth is composed of N spot-beams uniformly distributed over the coverage area as illustrated in Fig.1. Each beam makes use of the total available bandwidth $B = 500$ MHz and linear MMSE-based precoding is considered to mitigate the resulting inter-beam interference.

For each beam, K users are scheduled to held simultaneous transmission on the same PLFRAME. The received signal at the k-th user located at the n-th beam can be expressed as,

$$y_{k,n} = \mathbf{h}_{k,n}^T \mathbf{x} + n_{k,n}, \tag{1}$$

where $\mathbf{h}_{k,n} \in \mathbb{C}^{N\times 1}$ is the channel vector corresponding to user k scheduled in beam n, $\mathbf{x} \in \mathbb{C}^{N\times 1}$ represents the vector of N precoded symbols and $n_{k,n}$ is the zero-mean thermal noise seen by the user k of beam n with variance σ^2.

As discussed, we assume that MMSE-based precoding [5] is employed:

$$\mathbf{x} = \mathbf{W}_{\text{MMSE}} \cdot \mathbf{s}, \tag{2}$$

where $\mathbf{s}$ contains the non-precoded symbols coming from the DVB-S2 modulator with $\mathbb{E}\left[\mathbf{s}\mathbf{s}^H\right] = \mathbf{I}$. Note that the precoding matrix $\mathbf{W}_{\text{MMSE}}$ is $\mathbb{C}^{N\times N}$ and therefore, contains one precoding vector for each beam (or for each PLFRAME). The expression of $\mathbf{W}_{\text{MMSE}} \in \mathbb{C}^{N\times N}$ is given by,

$$\mathbf{W}_{\text{MMSE}} = \begin{bmatrix} \mathbf{w}_1 & \mathbf{w}_2 & \cdots & \mathbf{w}_N \end{bmatrix} \triangleq \eta \cdot \mathbf{W}, \tag{3}$$

with

$$\mathbf{W} = \tilde{\mathbf{H}}^H \left(\tilde{\mathbf{H}} \tilde{\mathbf{H}}^H + \alpha \mathbf{I} \right)^{-1}, \tag{4}$$

and $\alpha = \sigma^2 / P_{\text{beam}}$, being the regularization factor with P_{beam} the transmit power per beam. Note that $\tilde{\mathbf{H}}$ denotes the $N \times N$ channel matrix, which is a function of the original multicast (tall) channel matrix $\mathbf{H} \in \mathbb{C}^{KN\times N}$ (a detailed discussion is given in Section III). We apply the normalization factor η shown below to comply with the total power constraints of the satellite.

$$\eta = \sqrt{\frac{P_{total}}{\text{Trace}(\mathbf{W}\mathbf{W}^H)}}, \tag{5}$$

with P_{total} being the total satellite transmit power.

A. Channel Model

The complex channel coefficient of user k located in beam n is expressed as $h_{k,n} = |h_{k,n}|\, e^{j\angle h_{k,n}}$. Concerning the magnitude, this essentially includes propagation loss and antenna gains of the satellite transmit antenna and the UT's receiver antenna,

$$|h_{k,n}| = \frac{\lambda \sqrt{G_{k,\text{RX}}}\, |g_{k,n}|}{4\pi d_k} \tag{6}$$

where

- λ denotes the carrier wavelength in meters,
- $G_{k,\text{RX}}$ denotes the gain of the k-th UT,
- $|g_{k,n}|$ denotes the beam pattern gain,
- d_k denotes the slant range distance between the GEO satellite and the k-th UT.

Concerning the phase $\angle h_{k,n}$, we distinguish 3 components,

$$\angle h_{k,n} = \angle g_{k,n} + \psi_{\text{RF},k} + \psi_{\text{LNB},k}, \quad \text{[rad]} \tag{7}$$

where

- $\angle g_{k,n}$ denotes the phase of the complex channel coefficient (the antenna architecture introduces phase variations across the geographical coverage),
- $\psi_{\text{RF},k}$ refers to the phase rotation due to the RF signal propagation, which depends on the user-to-satellite distance as $2\pi d_k/\lambda$.
- $\psi_{\text{LNB},k}$ denotes the user-specific phase contribution which depends on the particular Low-Noise Block (LNB) deployed at the terminal. This is assumed to be Gaussian, with zero mean and a standard deviation of 0.24 degrees [20].

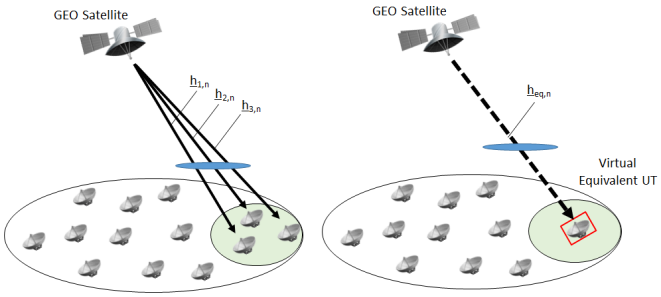

Fig. 2. (Left) Example of 1 beam with $K = 3$ multicasted users; (Right) Concept of equivalent multicast channel

For the sake of clarity on the analysis, we consider no time misalignment with respect to the symbol period (i.e., all the signals arrive at each UT at the same time instance) and perfect channel state information at the gateway side.

III. Equivalent Multicast Channel

In this section, we investigate the methodology to convert the multicast (tall) channel matrix $\mathbf{H} \in \mathbb{C}^{KN \times N}$, with number of rows equal to the number of scheduled users times the number of beams, into an equivalent square matrix $\tilde{\mathbf{H}} \in \mathbb{C}^{N \times N}$, where each group of K rows corresponding to the same beam has been replaced by an equivalent channel vector. The concept is illustrated in Fig. 2.

A. Virtual Equivalent UT (benchmark)

Herein, we consider a virtual equivalent UT for each multicast group, as depicted in Fig. 3. The virtual UT location for each beam is found by averaging the (latitude, longitude) coordinates of the multicasted users, so that the virtual UT is equidistant from the real UTs. Obviously, we do not have access to CSI measurements for the virtual UT. Therefore, we will use this method for benchmarking by assuming that we have access to the (perfect) CSI measurements of this virtual UT.

B. Average of phase and magnitude [15]

For illustration purposes, let us assume a multicast channel matrix $\mathbf{H} \in \mathbb{C}^{4\times 2}$, where $N = 2$ beams and $K = 2$ users are scheduled on each beam:

$$\mathbf{H} = \begin{bmatrix} |h_{11}|\, e^{j\angle(h_{11})} & |h_{12}|\, e^{j\angle(h_{12})} \\ |h_{21}|\, e^{j\angle(h_{21})} & |h_{22}|\, e^{j\angle(h_{22})} \\ |h_{31}|\, e^{j\angle(h_{31})} & |h_{32}|\, e^{j\angle(h_{32})} \\ |h_{41}|\, e^{j\angle(h_{41})} & |h_{42}|\, e^{j\angle(h_{42})} \end{bmatrix} \tag{8}$$

To convert $\mathbf{H} \in \mathbb{C}^{4\times 2}$ into $\tilde{\mathbf{H}} \in \mathbb{C}^{2\times 2}$, one could apply the arithmetic mean on the magnitude and on the phase [15] as follows,

$$\tilde{\mathbf{H}} = \begin{bmatrix} \frac{1}{2}\left(|h_{11}| + |h_{21}|\right) e^{j\frac{1}{2}(\angle(h_{11})+\angle(h_{21}))} & \frac{1}{2}\left(|h_{12}| + |h_{22}|\right) e^{j\frac{1}{2}(\angle(h_{12})+\angle(h_{22}))} \\ \frac{1}{2}\left(|h_{31}| + |h_{41}|\right) e^{j\frac{1}{2}(\angle(h_{31})+\angle(h_{41}))} & \frac{1}{2}\left(|h_{32}| + |h_{42}|\right) e^{j\frac{1}{2}(\angle(h_{32})+\angle(h_{42}))} \end{bmatrix} \tag{9}$$

By simply applying the arithmetic mean we have collapsed the channel vector of each multicasted group of users in into a single channel vector representing the equivalent multicast channel. However, [18] pointed out that the methodology in (9) breaks the phase structure of a real channel matrix (i.e. $\tilde{\mathbf{H}}$ no longer had a constant phase component across columns and a constant phase component across rows). As shown later, this will have an impact on the precoding performance.

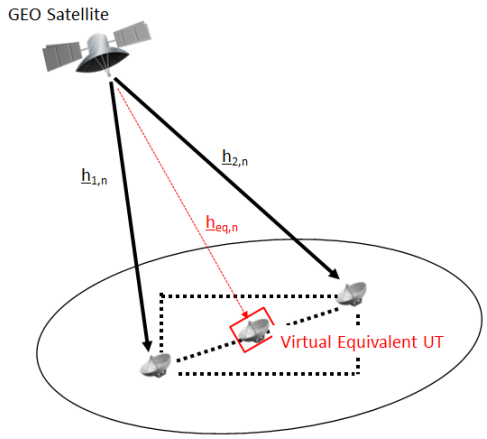

Fig. 3. Geographical Equivalent UT (upper-bound)

C. Average with Normalized Phase [18]

The authors of [18] proposed an arithmetic mean across the complex channel rows but considering a pre-processing step based on a phase normalization. Following the 4×2 example, and denoting the columns of the multicast (tall) channel matrix as $\mathbf{H} = \begin{bmatrix}\mathbf{h}_{1c} & \mathbf{h}_{2c} & \mathbf{h}_{3c} & \mathbf{h}_{4c}\end{bmatrix}$, the pre-processing step obtains an auxiliary matrix $\mathbf{H}_{\text{aux}} = \begin{bmatrix}\mathbf{h}_{1c,\text{aux}} & \mathbf{h}_{2c,\text{aux}} & \mathbf{h}_{3c,\text{aux}} & \mathbf{h}_{4c,\text{aux}}\end{bmatrix}$ with the following phase normalization,

$$\mathbf{h}_{ic,\text{aux}} = |\mathbf{h}_{ic}|\, e^{j\angle\left(\frac{\mathbf{h}_{ic}}{\mathbf{h}_{1c}}\right)}. \tag{10}$$

Once the phase normalization is done, matrix $\mathbf{H}_{\text{aux}}$ is used to perform the arithmetic mean directly on the rows corresponding to the users within a same multicast group.

D. Normalization of Relative Phase [19]

A new receiver architecture was proposed in the context of ESA Optimus project [19] which worked on differential phases of CSI components. Therefore, the following phased-normalized channel matrix was proposed:

$$\mathbf{H}_{\text{norm}} = \begin{bmatrix} |h_{11}| & |h_{12}|\, e^{j(\angle(h_{12})-\angle(h_{11}))} \\ |h_{21}| & |h_{22}|\, e^{j(\angle(h_{22})-\angle(h_{21}))} \\ |h_{31}|\, e^{j(\angle(h_{31})-\angle(h_{32}))} & |h_{32}| \\ |h_{41}|\, e^{j(\angle(h_{41})-\angle(h_{42}))} & |h_{42}| \end{bmatrix} \tag{11}$$

Then, the averaging proposed in (9) is applied to $\mathbf{H}_{\text{norm}}$. Note that the relative phase normalization is actually a conventional procedure performed by standard DVB-S2x receivers, which implement a phase tracking procedure with respect to the diagonal component.

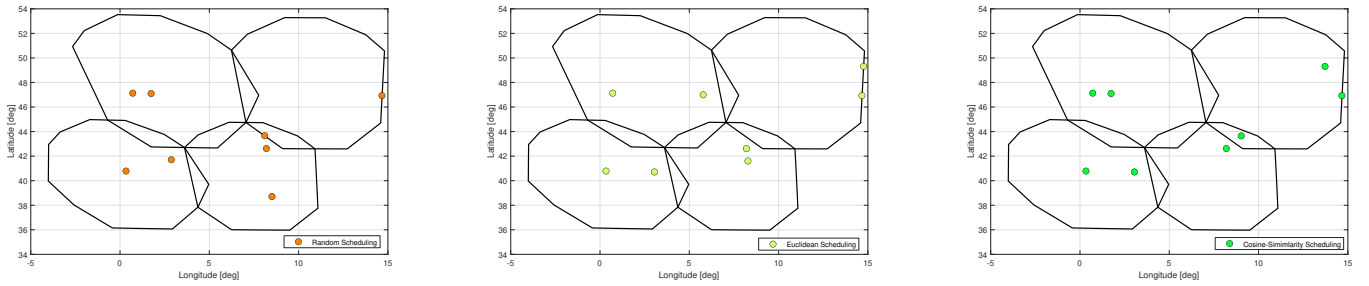

(a) Random scheduling (b) Euclidean-based scheduling (c) Cosine similarity based scheduling

Fig. 4. Zoom into 4 out of 108 beams to show an example of user scheduling for one particular time-slot with $K = 2$ users per beam

IV. Multicast User Scheduling

Following DVB-S2x implementation guideline, the multicast user scheduler shall be design to select UTs in a frame according to similarities on the SINR levels, which in general translate into similar channel conditions. To illustrate the impact of the multicast user scheduling (i.e. selection of users to share a PLFRAME) on the final precoding performance combined with the equivalent multicast channel, we consider 3 of the most popular scheduling strategies.

1) **Random Scheduling:** A K number of UTs per beam are selected uniformly at random.
2) **Euclidean-based or Geographical-based scheduling [16]:** UTs within beam n are selected based on certain similarity on their channel vectors. For this, we work with the following metric: $\|\mathbf{h}_{i,n} - \mathbf{h}_{j,n}\|_2$. When the two channel vectors are identical, this metric equals zero. Therefore, we schedule users within the same frame such that this metric is close to zero.
3) **Cosine-Similarity-based (same principle as in [14])**: Following the same intuition of the Euclidean-based scheduling, herein the similarity of the UTs' channel vectors is assessed with the cosine similarity metric, which is defined as,

$$\frac{\langle \mathbf{h}_{i,n}, \mathbf{h}_{j,n} \rangle}{\|\mathbf{h}_{i,n}\| \cdot \|\mathbf{h}_{j,n}\|}.$$

For real numbers, the above metric is between -1 and 1. However, for complex numbers, the above metrics gives a complex number without similarity meaning associated. Since we are dealing with complex channels, we make use of the following expression [21]:

$$\frac{1}{2} \frac{\langle \mathbf{h}_{i,n}, \mathbf{h}_{j,n} \rangle + \langle \mathbf{h}_{j,n}, \mathbf{h}_{i,n} \rangle}{\|\mathbf{h}_{i,n}\| \cdot \|\mathbf{h}_{j,n}\|} \in [-1, 1].$$

V. Numerical Evaluation

We consider the beam pattern shown in Fig. 1 with $N = 108$ beams. The beam pattern is obtained with an internal software from ESA, and corresponds to a Defocused Phased Array-Fed Reflector (DPAFR). The reflector size is of 2.2m and the array diameter of roughly 1.2m. The antenna array before the reflector is a circular array with 2λ spacing and 511 elements. The remaining simulation parameters are listed in Table I.

TABLE I
Simulation Parameters

Parameter	Value
Satellite Orbit	GEO 13E
Satellite Altitude	35786000 meters
EIRPSD per carrier	-27 dBW/Hz
Number of beams N	108
Beam Pattern	Fig. 1
Avg. beam gain on the beam center	44.4 dBi
Operational Frequency	19.95 GHz
Wavelength	0.015 meters
Bandwidth User Link	500 MHz
Bandwidth Margin	10% (resulting in 450 MHz)
Carrier Roll-Off	5% (resulting in 428.57 MHz)
Transmit Power per-beam	14.92 dBW
Boltzmann Constant	1.3806503e-23 J/K
Noise temperature at the antenna	50 K
Reference temperature	290 K
Noise Figure	2.278 dB
Noise Power	-118.3 dB
User Antenna Efficiency	0.6
User VSAT diameter	0.6 meter
User Antenna Gain	39.75 dBi

We assume that there are 25 UT per beam, from which $K \in [1, 2, 3]$ are scheduled at each time-instance. A total of 100 time-slots are averaged to obtain the results. Note that for each time instance the first scheduled user in each beam is selected with the random user scheduling. Only the additional multicasted users are selected following the scheduling strategies described in Section IV.

An example of user scheduling for one particular time-slot is shown in Fig. 4, where only a sub-set of 4 out of 108 beams is illustrated for the sake of clarity. The random scheme in Fig. 4(a) takes users at random while the other two schemes shown in Fig. 4(b) and Fig. 4(c) are shown to select users which tend to be close in geographical location, which is interpreted as an effort to schedule users with similar channel conditions.

Next, Fig. 5 compares the performance of the different equivalent multicast channel methodologies presented in Section III for different user scheduling strategies. For clarity purposes, Fig. 5(a) presents the results assuming a random user scheduling, Fig. 5(b) presents the results assuming the Euclidean-based scheduling, and Fig. 5(c) presents the same for the cosine similarity-based scheduling. All 3 sub-figures are illustrated with the same x-axis limits for the sake of

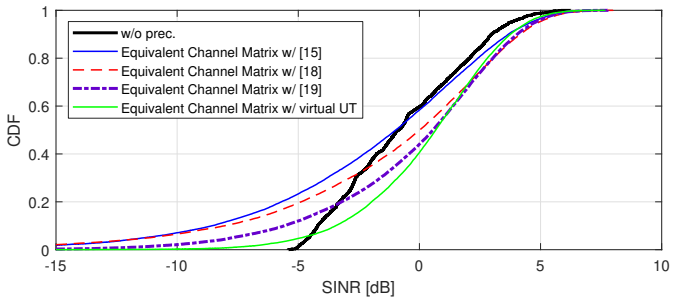

(a) Random scheduling

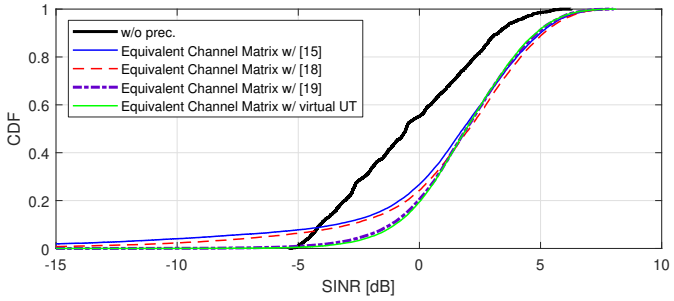

(b) Euclidean-based scheduling

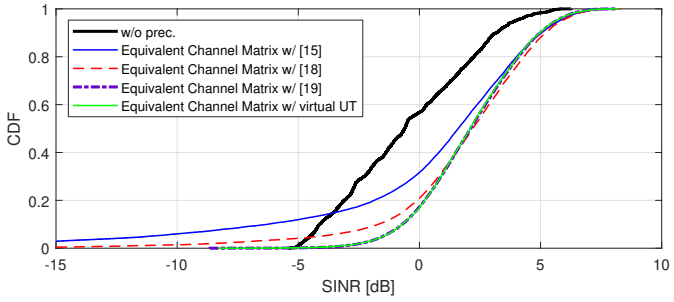

(c) Cosine similarity based scheduling

Fig. 5. Comparison of equivalent multicast channel methods

comparison. From Fig. 5 we conclude that: (1) Advanced scheduling techniques such as Euclidean-based or cosine similarity-based scheduling can push the multicast precoding performance to higher SINR levels; (2) The methodology used for computing the equivalent multicast channel plays a significant role in the final performance, being the technique in Section III-D [19] the one closer to the best possible performance (which is illustrated in Fig. 5 by the virtual UT presented in Section III-A); and (3) One can note that the methodologies for multicast equivalent channel calculation have a greater performance loss with respect to the upper-bound virtual UT when random users are scheduled. The message to take home from Fig. 5 is that not only the user scheduling is important but also the way the equivalent multicast channel is obtained. For a simplistic scheduling such as random user scheduling, $>$ 2.5dB can be gained only by selecting the appropriate equivalent multicast channel technique.

Assuming we use the equivalent multicast channel technique in Section III-D [19], Fig. 6 shows the performance in terms

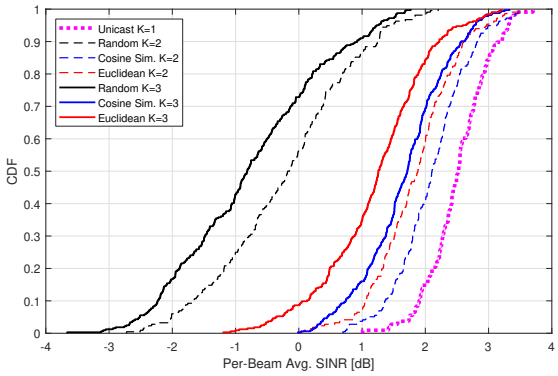

Fig. 6. Per-beam average SINR achieved with the equivalent multicast channel technique in Section III-D [19]

of per-beam average SINR achieved for the different user scheduling techniques and for different number of multiplexed users, i.e. unicast ($K = 1$), 2 users per frame ($K = 2$) and 3 users per frame ($K = 3$). It can be observed that: (1) The cosine similarity-based scheduling outperforms the other alternatives by providing higher per-beam average SINR; (2) As expected, multicast schemes always presents performance loss with respect to the unicast counterpart (and the more multicasted users, the more the performance loss). Regarding point (2), one should keep in mind that multicasting is a mandatory feature when dealing with GEO VHTS with typically few hundreds of users per beam. The methodologies presented in this paper show some implementation guidelines in terms of multicast scheduling and multicast equivalent channel to minimize the loss experienced due to multicasting.

VI. Conclusions and Remarks

This paper aimed to shed some light into the impact of combined user scheduling and equivalent multicast channel computation methodology into the final multicast precoding performance. After comparing the MMSE performance with respect to the different benchmark scheduling schemes, we can conclude the user scheduling has a strong impact when considering multicast precoding. It was found out that the cosine similarity-based scheduling (which takes into account both phase and magnitude of the channel vectors) is able to provide better performance that other scheduling strategies. When analyzing the user scheduling together with the different multicast equivalent channel computation techniques, it was observed that the combination of cosine similarity-based scheduling with the equivalent multicast channel technique in Section III-D [19] approaches the virtual UT approach, which can be considered the upper-bound in terms of performance. In general, the way the equivalent multicast channel is obtained can bring significant gains, particularly for simplistic scheduling schemes.

Acknowledgment

This work has been partially supported by the Luxembourg National Research Fund (FNR) under the project SmartSpace (C21/IS/16193290); and by the European Space Agency

(ESA) funded activity CGD: Prototype of a Centralized Broadband Gateway for Precoded Multi-beam Networks. Please note that the views of the authors of this paper do not necessarily reflect the views of ESA and/or SES.

REFERENCES

[1] "GEO HTS: Global reach with superior performance," https://www.ses.com/our-coverage/geo-hts, accessed: 2022-04.

[2] "Future Satellites: Expanding and renewing our satellite fleet," https://www.eutelsat.com/satellites/future-satellites.html, accessed: 2022-04.

[3] H. Fenech *et al.*, "Eutelsat HTS Systems," *International Journal of Satellite Communications and Networking (IJSCN)*, vol. 34, no. 4, pp. 503–521, 2016. [Online]. Available: https://onlinelibrary.wiley.com/doi/abs/10.1002/sat.1171

[4] P.-D. Arapoglou *et al.*, "DVB-S2X-enabled precoding for high throughput satellite systems," *International Journal of Satellite Communications and Networking (IJSCN)*, vol. 34, no. 3, pp. 439–455, 2016. [Online]. Available: https://onlinelibrary.wiley.com/doi/abs/10.1002/sat.1122

[5] M. A. Vazquez, A. Perez-Neira, D. Christopoulos, S. Chatzinotas, B. Ottersten, P. Arapoglou, A. Ginesi, and G. Taricco, "Precoding in Multibeam Satellite Communications: Present and Future Challenges," *IEEE Wireless Communications*, vol. 23, no. 6, pp. 88–95, December 2016.

[6] A. Wiesel, Y. Eldar, and S. Shamai, "Linear Precoding via Conic Optimization for Fixed MIMO Receivers," *IEEE Trans. Signal Process.*, vol. 54, no. 1, pp. 161–176, Jan. 2006.

[7] M. Bengtsson and B. Ottersten, *Book Chapter: Optimal and Suboptimal Transmit Beamforming* . CRC Press, 2001, ch. in Handbook of Antennas in Wireless Communications edited by L.C. Godara.

[8] P. Zetterberg and B. Ottersten, "The spectrum efficiency of a base station antenna array system for spatially selective transmission," *IEEE Transactions on Vehicular Technology*, vol. 44, no. 3, pp. 651–660, 1995.

[9] J. Krivochiza, J. C. M. Duncan, J. Querol, N. Maturo, L. M. Marrero, S. Andrenacci, J. Krause, and S. Chatzinotas, "End-to-end Precoding Validation over a Live GEO Satellite Forward Link," *IEEE Access*, pp. 1–1, 2021.

[10] P. J. Honnaiah, E. Lagunas, S. Chatzinotas, and J. Krause, "Interference-aware demand-based user scheduling in precoded high throughput satellite systems," *IEEE Open Journal of Vehicular Technology*, vol. 3, pp. 120–137, 2022.

[11] K.-U. Storek, R. T. Schwarz, and A. Knopp, "Multi-satellite multi-user mimo precoding: Testbed and field trial," in *ICC 2020 - 2020 IEEE International Conference on Communications (ICC)*, 2020, pp. 1–7.

[12] E. Lagunas, A. Pérez-Neira, M. Martínez, M. A. Lagunas, M. A. Vázquez, and B. Ottersten, "Precoding With Received-Interference Power Control for Multibeam Satellite Communication Systems," *Frontiers in Space Technologies*, vol. 2, 2021. [Online]. Available: https://www.frontiersin.org/article/10.3389/frspt.2021.662883

[13] Taesang Yoo and A. Goldsmith, "On the optimality of multiantenna broadcast scheduling using zero-forcing beamforming," *IEEE Journal on Selected Areas in Communications*, vol. 24, no. 3, pp. 528–541, March 2006.

[14] D. Christopoulos, S. Chatzinotas, and B. Ottersten, "Multicast multigroup precoding and user scheduling for frame-based satellite communications," *IEEE Transactions on Wireless Communications*, vol. 14, no. 9, pp. 4695–4707, Sep. 2015.

[15] E. Lagunas, S. Andrenacci, S. Chatzinotas, and B. Ottersten, "Cross-Layer Forward Packet Scheduling for Emerging Precoded Broadband Multibeam Satellite System," in *Advanced Satellite Multimedia Systems Conference (ASMS)*, Sep. 2018, pp. 1–8.

[16] G. Taricco, "Linear precoding methods for multi-beam broadband satellite systems," in *European Wireless 2014; 20th European Wireless Conference*, May 2014, pp. 1–6.

[17] A. Guidotti and A. Vanelli-Coralli, "Clustering strategies for multicast precoding in multibeam satellite systems," *International Journal of Satellite Communications and Networking*, vol. 38, no. 2, pp. 85–104, 2020. [Online]. Available: https://onlinelibrary.wiley.com/doi/abs/10.1002/sat.1312

[18] X. Artiga and M. n. Vázquez, "Effects of channel phase in multibeam multicast satellite precoding systems," in *Advances in Communications Satellite Systems. Proceedings of the 37th International Communications Satellite Systems Conference (ICSSC-2019)*, 2019, pp. 1–12.

[19] ESA OPTIMUS Project: COptimized transmission techniques for satcom unicast interactive traffic . [Online]. Available: https://wwwfr.uni.lu/snt/research/sigcom/projects/optimus_optimized_transmission_techniques_for_satcom_unicast_interactive_traffic

[20] A. I. Perez-Neira, M. A. Vazquez, M. B. Shankar, S. Maleki, and S. Chatzinotas, "Signal Processing for High-Throughput Satellites: Challenges in New Interference-Limited Scenarios," *IEEE Signal Processing Magazine*, vol. 36, no. 4, pp. 112–131, 2019.

[21] Linear Algebra Course at Clark University. [Online]. Available: https://mathcs.clarku.edu/~ma130/